

Tunable variation of the electron effective mass and exciton radius in hydrogenated GaAs_{1-x}N_x

A. Polimeni,* G. Baldassarri Höger von Högersthal, F. Masia, A. Frova, and M. Capizzi
INFN and Dipartimento di Fisica, Università di Roma "La Sapienza," Piazzale A. Moro 2, I-00185 Roma, Italy

Simone Sanna and Vincenzo Fiorentini
INFN-Dipartimento di Fisica, Università di Cagliari, Cittadella Universitaria, I-09042 Monserrato, Italy

P. J. Klar and W. Stolz
Department of Physics and Material Sciences Center, Philipps-University, Renthof 5, D-35032 Marburg, Germany
 (Received 26 August 2003; published 7 January 2004)

Magnetophotoluminescence measurements show that the electron effective mass and the exciton radius in hydrogen irradiated GaAs_{1-x}N_x vary continuously as a function of the hydrogen dose until they recover the values of N-free GaAs. First-principles calculations account for the experimental findings through the formation of a specific N-dihydrogen complex, which leads to the removal of the electron localization caused by N incorporation into GaAs.

DOI: 10.1103/PhysRevB.69.041201

PACS number(s): 71.55.Eq, 61.72.Bb, 71.35.Ji

Random alloys, which lack translational symmetry, can be described often in terms of translational symmetry-derived concepts such as the band structure and carrier effective mass. The crystal potential, $V(x)$, of an AB_xC_{1-x} alloy can be expressed by a linear interpolation of those of the binary constituents, i.e., $V(x) = x \cdot V_{AB} + (1-x) \cdot V_{AC}$. This “virtual crystal approximation” works in many materials (e.g., Al_xGa_{1-x}As), where disorder is usually rationalized through weak quadratic composition dependencies of the alloy properties. On the contrary, no variant of a suitably corrected virtual-crystal description seems viable in the case of GaAs_{1-x}N_x,¹ where the incorporation of a small amount of N (~1%) leads to a huge, nonlinear decrease in the band gap and a large variation in the electron effective mass²⁻⁶ and exciton radius.⁷

In this paper, we use photoluminescence (PL) under a magnetic field B to investigate the effects of *ex situ* hydrogen incorporation on the bottom of the conduction band (both curvature and localized character degree) of a GaAs_{1-x}N_x alloy with $x=0.1\%$. By exploiting the B -induced energy shift of the free-electron to neutral-carbon recombination we measure directly the electron effective mass, m_e^* . We find that m_e^* decreases continuously from the GaAs_{1-x}N_x value to that of GaAs with increasing H dose. By studying the diamagnetic shift of the free-exciton energy, we determine independently the exciton wave function size, r_{exc} , which increases with H irradiation dose. Therefore, the increase in m_e^* and decrease in r_{exc} with N in GaAs_{1-x}N_x are effectively and fully counteracted by H incorporation. Finally, first-principles calculations show that H irradiation of GaAs_{1-x}N_x causes the conduction band to essentially recover the delocalized character of N-free GaAs.

The GaAs_{1-x}N_x sample investigated has been grown by metal-organic vapor-phase epitaxy on a (100)-oriented GaAs substrate. The GaAs_{1-x}N_x thickness (0.5 μm) and composition ($x=0.1\%$) have been determined by x-ray diffraction measurements. The sample has been hydrogenated at 300 °C

by a low-energy ion gun (beam energy ~100 eV). Different H doses have been employed ($d_{\text{H}} = 1.0 \times 10^{18} - 5.0 \times 10^{18}$ ions/cm²). PL measurements have been carried out at a temperature $T=30$ K using a neodymium-vanadate laser (laser wavelength 532 nm) as the excitation source. PL has been recorded under a magnetic field ($B=0-12$ T) and spectrally analyzed by a single-grating 0.75-m-long monochromator coupled to an InGaAs linear array cooled at -105 °C (the spectral resolution is 0.1 nm). The energetics and electronic properties of hydrogenated GaAs_{1-x}N_x have been calculated within local density-functional theory using the all-electron projector-augmented-wave method⁸ as implemented in the VASP code.⁹

Let us describe first the PL spectra of the GaAs_{1-x}N_x alloy shown in Fig. 1 for different H doses, d_{H} 's. The H-free sample displays several recombination lines (see bottommost continuous curve). The low energy features (below 1.462 eV) in the PL spectrum are ascribed to impuritylike states arising from nitrogen pairs and higher order clusters.¹⁰ The bands located at higher energy (above 1.462 eV) are related, instead, to radiative recombinations involving extended states of the GaAs_{1-x}N_x lattice. The PL band at 1.469 eV is attributed to a free-electron to neutral-carbon transition (e, C) (Ref. 11) on the grounds of its behavior with temperature and laser power (not shown here). On the same ground, the PL band located at the highest energy (1.480 eV) is due to free exciton recombination from the GaAs_{1-x}N_x band gap, hereafter called E_- [see inset in Fig. 1, which depicts both the (e, C) and E_- transitions in a single particle scheme]. As previously reported,² H irradiation leads first to a passivation of the N cluster states and then to an apparent reopening of the GaAs_{1-x}N_x band gap toward that of the GaAs reference (topmost continuous curve). As a matter of fact, both the (e, C) and the E_- recombination bands converge to those of the GaAs reference, as shown by continuous lines in Fig. 1. With applying a magnetic field (see dashed curves in Fig. 1), all PL lines below 1.462 eV in the

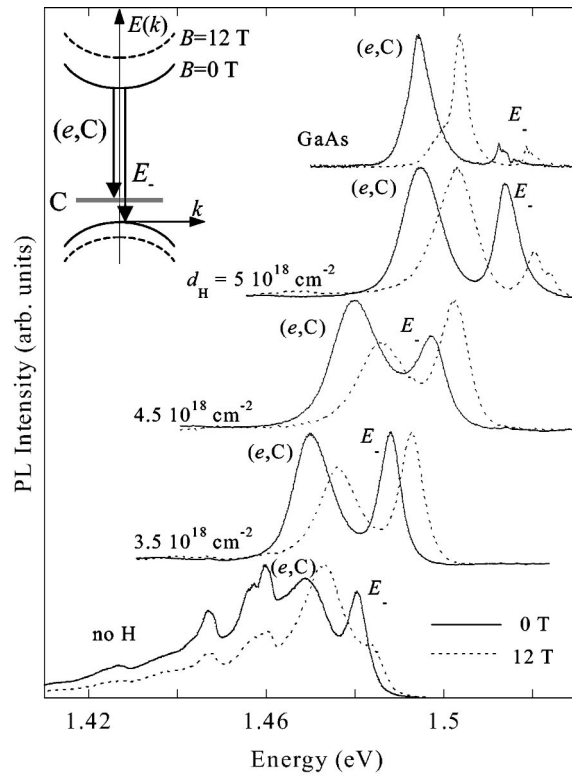


FIG. 1. PL spectra of a $\text{GaAs}_{0.999}\text{N}_{0.001}$ alloy treated with different hydrogen doses d_H . Measurements have been performed at about $T=30$ K to reduce the contribution from possible N-related localized state and donor-acceptor pair recombination. The bottom-most and topmost spectra refer to an untreated $\text{GaAs}_{1-x}\text{N}_x$ and a reference GaAs sample, respectively. Continuous and dashed lines indicate PL spectra taken under zero and 12-T magnetic fields, respectively. (e,C) indicates the free-electron to neutral-carbon recombination and E_- indicates the free-exciton recombination. The inset sketches these recombinations in a reciprocal space scheme at $k \sim 0$. Different laser power densities have been employed for the different samples in order to highlight the presence of both (e,C) and E_- bands.

H-free sample remain pinned in energy, consistently with the highly localized nature expected for N cluster states. On the contrary, the E_- and (e,C) bands blue shift with increasing B . Notice that the energy separation between these two transitions increases on going from the H-free to the H-treated samples, due to a corresponding decrease in the tensile strain with decreasing the effective N concentration.¹² Indeed, for decreasing N concentration the top of the valence band acquires a more pronounced heavy hole character and, in turn, the binding energy of the acceptor impurity increases.

The energy shift ΔE_d of the (e,C) and E_- recombination lines are shown as a function of B in Figs. 2(a) and 2(b), respectively, for $\text{GaAs}_{1-x}\text{N}_x$ (both untreated and hydrogenated, full symbols) and for the GaAs reference (open symbols). The E_- band shifts with B at a lower rate than the (e,C) band does, owing to the larger Coulomb attraction between the electron and hole in the former case. We exploit the (e,C) energy shift to derive the electron effective mass in $\text{GaAs}_{1-x}\text{N}_x$ for different d_H values as explained in the following. In the inset of Fig. 1 the C-related level stays fixed in

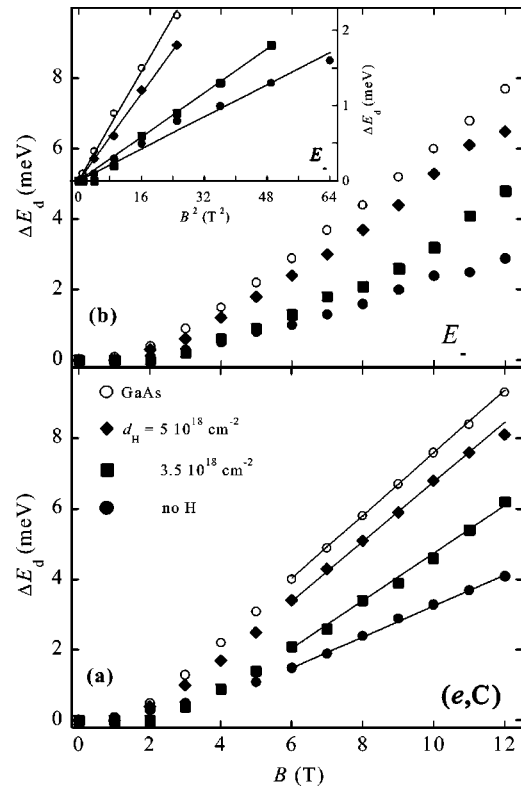


FIG. 2. (a) Energy shift with magnetic field of the free-electron to neutral-carbon recombination (e,C) for some of the samples shown in Fig. 1. The continuous lines are fits to the data by $\Delta E_d = (\hbar e/2m_e^*)B$. The electron effective mass m_e^* is derived directly from the line slope. (b) Energy shift with magnetic field of the free-exciton recombination E_- . The samples considered are the same as in (a). The inset highlights the low-field part of the graph and it displays the E_- energy dependence on B^2 . The straight lines are fits to the data through $\Delta E_d = [e^2 \langle r_{eh}^2 \rangle / (8\mu)]B^2$, where $\langle r_{eh}^2 \rangle$ is a fit parameter.

energy, as reported in Ref. 13, while the conduction band bottom and the valence band top shift upon application of B . Therefore, in this approximation the shift of the (e,C) transition is ascribed entirely to the shift of the conduction band bottom. Continuous lines in Fig. 2(a) are a fit of the formula for the magnetic field dependence of the bottommost Landau level of the conduction band, $\Delta E_d = (\hbar e/2m_e^*)B$, to the (e,C) shift in the B -linear region of ΔE_d .¹³ At zero magnetic field, ΔE_d extrapolates to a negative value, of order of $k_B T/2$, as found in other magneto-PL measurements of the B -induced shift of free-electron to neutral-acceptor recombinations.¹⁴ This behavior is usually attributed to the change in the density of states of the system from three to one dimensional due to the applied magnetic field. The slope of the fitting curve increases with increasing H dose until the value of the GaAs reference is obtained. The diamagnetic shift of the E_- excitonic transition can be modeled at low field in the small perturbation limit. The inset of Fig. 2(a) shows a fit of $\Delta E_d = [e^2 \langle r_{eh}^2 \rangle / (8\mu)]B^2$ to the E_- data in the quadratic low-field region. r_{eh} and μ are, respectively, the electron-hole distance and reduced effective mass of the exciton, and $\langle r_{eh}^2 \rangle$ is the expectation value of r_{eh}^2 on the unperturbed (zero field)

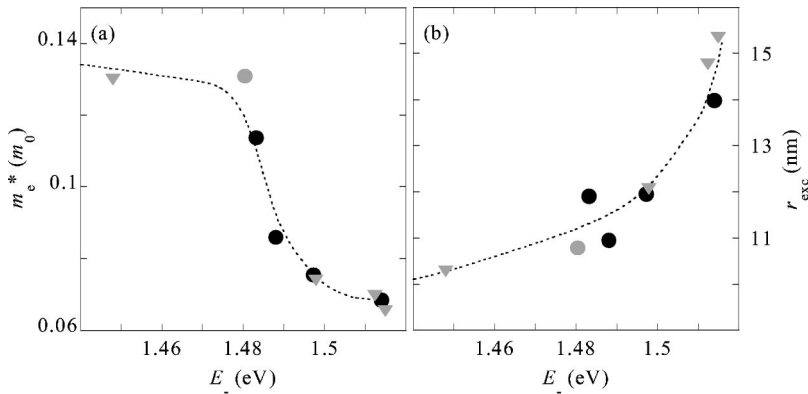


FIG. 3. (a) Electron effective mass dependence on the free-exciton peak energy as measured at 10 K. Full dots refer to the untreated (gray) and hydrogenated (black) GaAs_{0.999}N_{0.001} samples considered in this work, gray triangles refer to GaAs_{1-x}N_x alloys with different x values. (b) Exciton size dependence on the free-exciton peak energy at 10 K. Symbols have the same meaning as in part (a). The sample with $m_e^* = 0.11m_0$ and $r_{\text{exc}} = 11.9$ nm whose spectrum is not shown in Fig. 1 is an hydrogenated sample with $d_{\text{H}} = 1.0 \times 10^{18} \text{ cm}^{-2}$. Dashed lines are guides to the eye.

eigenstate. An estimate of $r_{\text{exc}} = \sqrt{\langle r_{\text{eh}}^2 \rangle}$ for each sample can be obtained by using the m_e^* values derived from the (e, C) shift. The hole mass values, m_h , used in μ are derived by setting $m_h = 0.45m_0$ (where m_0 is the vacuum electron mass) for the GaAs reference¹⁵ and scaling m_h according to the variation of the acceptor binding energy due to the change of strain with effective N concentration.¹² Consistently with the H-induced m_e^* decrease, the exciton size increases upon hydrogenation, thus indicating a sizable change in the conduction band shape.

Figures 3(a) and 3(b) show, respectively, the electron effective mass and exciton size as a function of E_- . Full dots refer to the GaAs_{1-x}N_x alloy with $x = 0.1\%$ for both the untreated sample (gray symbol) and the hydrogenated ones (black symbols). Gray full triangles are the m_e^* and r_{exc} values measured in not hydrogenated samples with different N concentration ($x = 0$, $x < 0.043\%$, $x = 0.043\%$ and 0.21%) by using the same methods described above.⁷ Both m_e^* and r_{exc} vary biuniquely with sample emission energy, namely, they depend on the *effective* N concentration in the crystal regardless of how this has been achieved (either by N incorporation in GaAs or by H irradiation in GaAs_{1-x}N_x). These findings allow monitoring the evolution of the electronic properties of GaAs_{1-x}N_x in a virtually continuous manner and well support the sudden change in m_e^* and r_{exc} for $x \sim 0.1\%$ found in Ref. 7. Indeed, the electron effective mass increases very rapidly from the GaAs value ($= 0.065m_0$ as derived here) to $0.09m_0$ for $E_- \sim 1.49$ eV and reaches a value of $\sim 0.13m_0$ for $E_- \sim 1.45$ eV. Accordingly, the exciton size undergoes a shrinking with increasing the N effective concentration and varies from $r_{\text{exc}} = 15.3$ nm in GaAs to 10.3 nm in GaAs_{0.998}N_{0.002}.¹⁶ We point out that an almost full recovery of the GaAs m_e^* and r_{exc} has been found in the other samples investigated. These samples have both lower ($x = 0.043\%$) and higher ($x = 0.21\%$) N concentrations and have been irradiated with a H dose such to produce a nearly full recovery of the GaAs band gap.

We have shown that the electron effective mass and exciton radius in GaAs_{1-x}N_x are transformed back to those of GaAs by H incorporation. Previous theoretical works have indicated that the formation of a specific N-dihydride (N-H₂^{*}) complex in GaAs_{1-x}N_x effectively removes the strong potential mismatch between N and As as seen by neighboring Ga orbitals.¹⁷⁻²⁰ In this complex, one H is

bound to N in the antibonding site and the other H is in a bond-center position, bound to a Ga atom nearest neighbor of N. This leads to the saturation of the deep N potential and the removal of N-induced states from the band gap. Here, local-density-functional calculations show that the same N-H₂^{*} complex also affects the carrier localization degree and conduction band shape. An epitaxial GaAs_{1-x}N_x layer grown on GaAs has been simulated by a 64-atom GaAs supercell with one As-substituting N. The N concentration is $x = 0.03$, lower concentrations being computationally impractical. Both in H-containing and H-free GaAs_{1-x}N_x the lattice constant along the growth direction and the atomic geometries were optimized, and the band structure and charge densities calculated (full details will be published elsewhere). Part (a) of Fig. 4 depicts the difference of the total charge densities calculated with and without an excess electron, namely, the charge density of an added electron in a H-free GaAs_{1-x}N_x crystal. The excess electron in the conduction band is clearly localized along the Ga-N bonds in agreement with previous calculations in a similar N concentration range.²¹ Part (b) of Fig. 4 shows the same quantities calculated for a GaAs_{1-x}N_x alloy in which the N-H₂^{*} complex is formed. A delocalization of the excess electron can be observed in this case, consistently with the increase in r_{exc} and decrease in m_e^* here measured at smaller x . These findings are confirmed by the very similar effective masses cal-

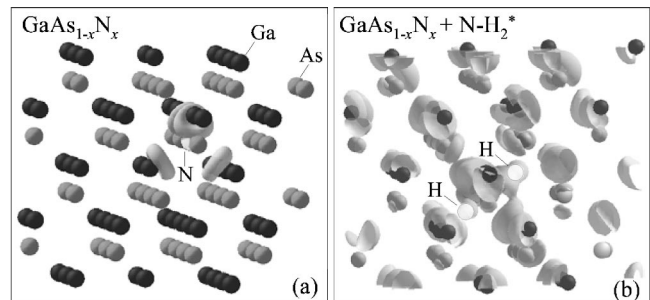


FIG. 4. (a) Calculated charge isosurfaces for an electron added to a neutral 64-atom GaAs_{0.97}N_{0.03} supercell without H. Light and dark gray balls indicate As and Ga atoms, respectively. Note the charge density accumulation around the N atom (figure center). (b) Same as (a) for a GaAs_{0.97}N_{0.03} lattice in which a N-H₂^{*} (see the text) complex is formed. H atoms are indicated by pale gray balls in the figure center.

culated at Γ for hydrogenated $\text{GaAs}_{0.97}\text{N}_{0.03}$ ($0.07m_0$) and GaAs ($0.06m_0$), and by the almost identical band structures in the two cases.²²

Previous and present results show that hydrogen in $\text{GaAs}_{1-x}\text{N}_x$ modifies in a controlled manner the energy,² the dependence on temperature²³ and pressure²⁴ of the band gap, the lattice constant,¹² and, lastly, the electron effective mass and exciton radius. Therefore, one can argue that hydrogen neutralizes the strong potential introduced by N to such an extent to render it indistinguishable from the As atomic potential.

In conclusion, we showed by magneto-PL that the band gap widening induced by H in $\text{GaAs}_{1-x}\text{N}_x$ maps on a strong modification in the conduction band curvature and degree of exciton localization. Indeed, the increase in m_e^* and decrease in r_{exc} with x are counteracted by H incorporation, which

effectively and in a tuneable manner re-establishes the band gap and conduction band properties of GaAs . Density-functional calculations indicate that the localization of conduction electrons near N in $\text{GaAs}_{1-x}\text{N}_x$ is removed upon the formation of a N-H_2^* complex, leading to very similar conduction band shapes and masses for GaAs and hydrogenated $\text{GaAs}_{1-x}\text{N}_x$. Therefore, our findings demonstrate that the *local* interaction of H with N in $\text{GaAs}_{1-x}\text{N}_x$ has profound consequences on several properties of the *extended* states of the crystal and not only on its band gap energy.

This work was funded by Progetto Giovani Ricercatori, COFIN 2001 (MIUR), and the Deutsche Forschungsgemeinschaft. Theoretical work was supported partly by Parallel Supercomputing Initiative of INFN and by CNR Agenzia2000. We acknowledge A. Miriametro and L. Ruggieri for technical assistance.

*Email address: polimeni@roma1.infn.it

¹L.-W. Wang, L. Bellaiche, S.-H. Wei, and A. Zunger, *Phys. Rev. Lett.* **80**, 4725 (1998).

²For a review see *III-N-V Semiconductor Alloys*, special issue of *Semicond. Sci. Technol.* **17**, 741 (2002).

³P. N. Hai, W. M. Chen, I. A. Buyanova, H. P. Xin, and C. W. Tu, *Appl. Phys. Lett.* **77**, 1843 (2000).

⁴Y. Zhang, A. Mascharenas, H. P. Xin, and C. W. Tu, *Phys. Rev. B* **61**, 7479 (2000).

⁵J. Wu, W. Shan, W. Walukiewicz, K. M. Yu, J. W. Ager III, E. E. Haller, H. P. Xin, and C. W. Tu, *Phys. Rev. B* **64**, 085320 (2001).

⁶D. L. Young, J. F. Geisz, and T. J. Coutts, *Appl. Phys. Lett.* **82**, 1236 (2003).

⁷F. Masia, A. Polimeni, G. Baldassarri, M. Capizzi, P. J. Klar, and W. Stolz, *Appl. Phys. Lett.* **82**, 4474 (2003).

⁸P. Blöchl, *Phys. Rev. B* **50**, 17 953 (1994).

⁹G. Kresse and J. Furthmüller, *Phys. Rev. B* **54**, 11 169 (1996); G. Kresse and D. Joubert, *ibid.* **59**, 1758 (1999).

¹⁰P. J. Klar, H. Grüning, W. Heimbrod, J. Koch, F. Höhnsdorf, W. Stolz, P. M. A. Vicente, and J. Camassel, *Appl. Phys. Lett.* **76**, 3439 (2000).

¹¹T. Makimoto, H. Saito, T. Nishida, and N. Kobayashi, *Appl. Phys. Lett.* **70**, 2984 (1997).

¹²A. Polimeni, G. Ciatto, L. Ortega, F. Jiang, F. Boscherini, F. Filippone, A. Amore Bonapasta, M. Stavola, and M. Capizzi, *Phys. Rev. B* **68**, 085204 (2003).

¹³J. A. Rossi, C. M. Wolfe, and J. O. Dimmock, *Phys. Rev. Lett.* **25**, 1614 (1970).

¹⁴W. Rühle and E. Göbel, *Phys. Status Solidi B* **78**, 311 (1976); P. J. Dean, H. Venghaus, and P. E. Simmonds, *Phys. Rev. B* **18**, 6813 (1978); S. Zemon, P. Norris, E. S. Koteles, and G. Lambert, *J. Appl. Phys.* **59**, 2828 (1986).

¹⁵I. Vurgaftman, J. R. Meyer, and L. R. Ram-Mohan, *J. Appl. Phys.* **89**, 5815 (2001).

¹⁶We point out that this method provides a sound value of both m_e^* and r_{exc} (corresponding to an exciton Bohr radius $a_0^{\text{exc}} = r_{\text{exc}}/\sqrt{3} = 8.8$ nm) for the GaAs reference.

¹⁷Yong-Sung Kim and K. J. Chang, *Phys. Rev. B* **66**, 073313 (2002).

¹⁸A. Janotti, S. B. Zhang, Su-Huai Wei, and C. G. Van de Walle, *Phys. Rev. Lett.* **89**, 086403 (2002).

¹⁹A. Amore Bonapasta, F. Filippone, P. Giannozzi, M. Capizzi, and A. Polimeni, *Phys. Rev. Lett.* **89**, 216401 (2002).

²⁰W. Orellana and A. C. Ferraz, *Appl. Phys. Lett.* **81**, 3816 (2002).

²¹T. Mattila, Su-Huai Wei, and A. Zunger, *Phys. Rev. B* **60**, R11245 (1999).

²²For pristine $\text{GaAs}_{1-x}\text{N}_x$ the bands are entirely different, with a dispersed state dipping below the conduction edge. The effective mass cannot be evaluated reliably because of the incipient coupling with valence bands due to the local density approximation gap underestimation.

²³A. Polimeni, M. Bissiri, A. Augieri, G. Baldassarri Höger von Högersthal, M. Capizzi, D. Gollub, M. Fischer, M. Reinhardt, and A. Forchel, *Phys. Rev. B* **65**, 235325 (2002).

²⁴P. J. Klar *et al.* (unpublished).